Journal of Medicinal Chemistry

Article

pubs.acs.org/jmc

Synthesis and Biological Evaluation of Novel Millepachine Derivatives As a New Class of Tubulin Polymerization Inhibitors

Zhuang Yang,[†,‡,∥] Wenshuang Wu,[†,∥] Jingjing Wang,[†,∥] Li Liu,[‡] Luyuan Li,[§] Jianhong Yang,[†] Guangcheng Wang,[†] Dong Cao,[†] Ronghong Zhang,[†] Minghai Tang,[†] Jiaolin Wen,[†] Jun Zhu,[†] Wei Xiang,[†] Fang Wang,[†] Liang Ma,[†] Mingli Xiang,[†] Jingsong You,[‡] and Lijuan Chen*[,†]

[†]State Key Laboratory of Biotherapy/Collaborative Innovation Center of Biotherapy and Cancer Center, West China Hospital of Sichuan University, Chengdu, China

[‡]College of Chemistry, Sichuan University, Chengdu, China

[§]State Key Laboratory of Medicinal Chemical Biology and College of Pharmacy, Nankai University, Tianjin, China

ABSTRACT: Twenty-one novel derivatives of millepachine were synthesized and evaluated for their in vitro antiproliferative activity. Among them, **8** exhibited the most potent activity, with IC_{50} values of 8−27 nM against panel of cancer cell lines and retained full activity in multidrug resistant cancer cells. Treated cells were arrested in G2/M phase and resulted in cellular apoptosis. Microtubule dynamics confirmed **8** was a novel tubulin polymerization inhibitor by binding at the colchicine site. **8** also exhibited antivascular activity because it concentration dependently reduced the cell migration and disrupted capillary like tube formation in HUVEC cells. Furthermore, the hydrochloride salt of **8** (**8·HCl**) significantly improved the bioavailability up to 47% while retaining the antiproliferative activity. Importantly, **8·HCl** significantly inhibited tumor growths in four xenograft models including resistance tumor-cell-bearing mice models without causing significant loss of body weight, suggesting that **8** is a promising new orally anticancer agent to be developed.

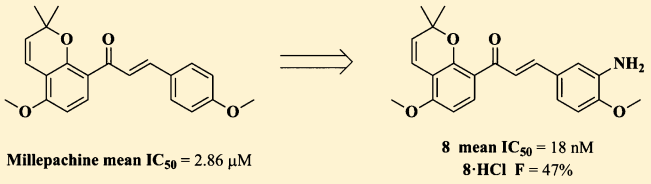

INTRODUCTION

Microtubules, as key components of the cytoskeleton, play important roles in a series of cellular processes such as regulation of motility, cell signaling, formation and maintenance of cell shape, secretion, and intracellular transport.[1−3] Because of the important roles of microtubules for the life cycle of the cell, the discovery and development of small molecules which act on tubulin to interfere with the dynamic of tubulin polymerization to therapy cancer has been a continuing interest.[4,5] In the past decades, numbers of small molecules derived from natural sources or obtained by chemical synthesis have been reported.[6] These compounds were divided into three major groups: the taxane site[7] for microtubule-stabilizing agents, the *vinca* site,[7,8] and the colchicine site[9] for microtubule polymerization inhibitors. Nevertheless, the clinical using of these compounds was always limited by the high toxicity, marginal oral bioavailability, poor solubility, complex synthesis, and drug resistance.[10] Therefore, searching and synthesizing low molecular weight compounds with high oral bioavailability and potent antitumor activity for first and second line therapy is urgently needed.

Millepachine, a novel chalcone with a 2,2-dimethylbenzopyran motif (**1**, Chart 1), was first isolated from the *Millettia pachycarpa* by our group and reported to have potent cytotoxic against a variety of human cancer cells, with IC_{50} values ranging from 1.51 to 4.0 μM and potent in vivo antitumor activity.[11] In an effort to further improve the antiproliferative activity of millepachine, we have explored the B-ring of millepachine with different substituted groups, for example, replacement methoxyl with diethyl amino or introduction of hydroxyl group on the B-ring of millepachine resulted in improvement on antiproliferative activity and in vivo effect.[12−15] Among the synthesized compounds, the most active compound **2**, which introduced a propionate ester substituted at the *ortho*-position of methoxy group on the B-ring, was 15−45-fold more active than millepachine as an tubulin de-polymerization inhibitor.[12] However, the pharmacokinetic studies showed that the bioavailability of **2** was 27%, which limited further study. To find more effective and high bioavailability compounds, we designed and synthesized a series of amino derivatives of millepachine using the bioisosteric rule between hydroxyl group and amino group and the amino groups at the *ortho*-position of methoxyl group on the B-ring.

In the present study, we examined the efficacy of the newly synthesized 21 compounds with three kinds of cancer cell lines. Compound **8** showed the most potent activity with IC_{50}s between 8 and 26 nM in a panel of tumor cell lines and also showed promising activities in drug-resistant tumor cells. Interestingly, we found that **8** was a tubulin polymerization inhibitor by binding at the colchicine site and showed higher antitubulin polymerization activity than colchicine. The

Received: June 4, 2014
Published: September 10, 2014

Chart 1. Chemical Structures of Millepachine and SAR Modifications

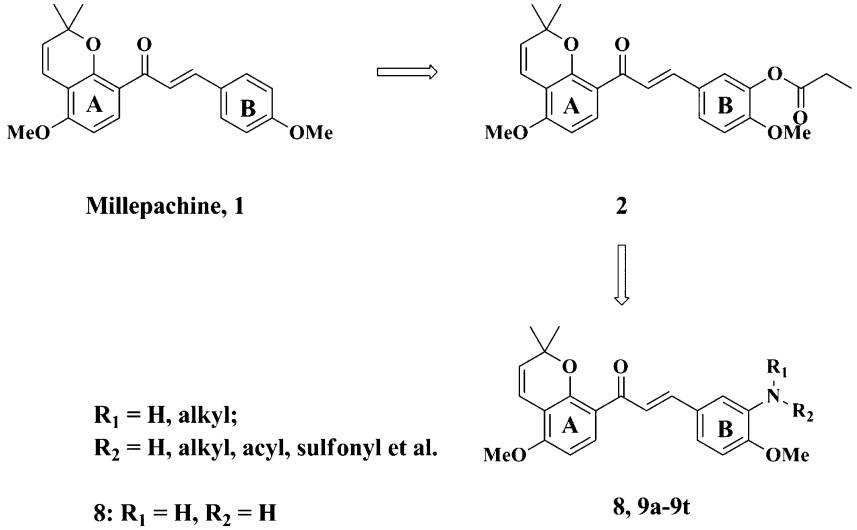

Scheme 1. Synthesis of the Derivatives of Millepachine[a]

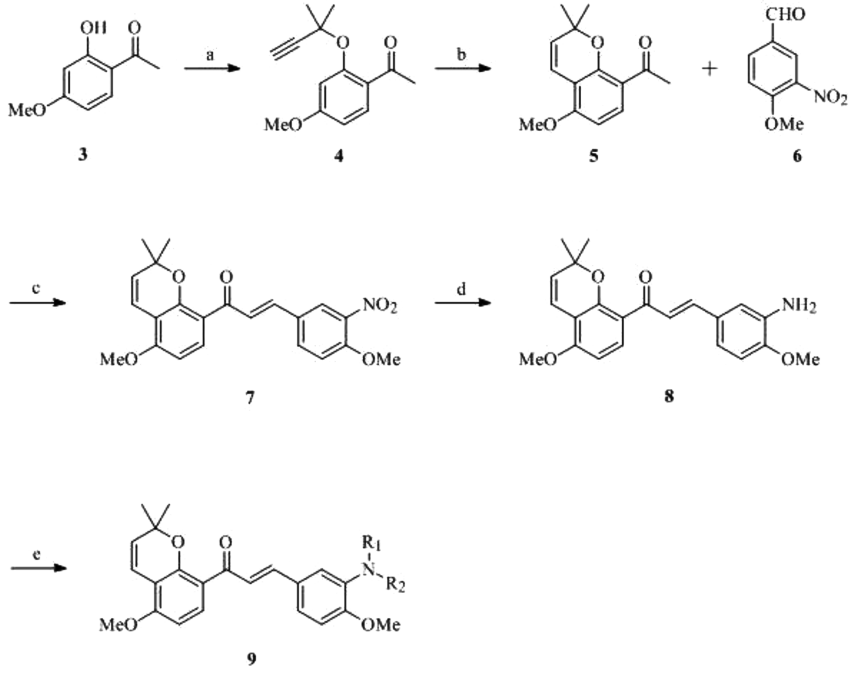

[a]Reagents and conditions: (a) 3-Chloro-3-methylbut-1-yne, $CuCl_2 \cdot 2H_2O$, DBU, CH_3CN, 0 °C, 5 h. (b) Pyridine, 120 °C, 12 h. (c) KOH (50% w/v aqueous solution), CH_3OH, rt, 12 h. (d) Fe powder, NH_4Cl, CH_3CH_2OH/H_2O (3:1, v/v), 80 °C. (e) Method A for **9a**–**9g**, K_2CO_3, RX, CH_3CN, reflux, 6 h; method B for **9h**–**9l** and **9n**, RCOOH, EDCI, DMAP, CH_2Cl_2, rt, 12 h; method C for **9m**, KOCN, AcOH/H_2O, rt, overnight; method D for **9o**–**9r**, RSO_2Cl, Et_3N, CH_2Cl_2, rt, 6 h; method E for **9s** and **9t**, a, method A; b, CH_2Cl_2/CF_3COOH, rt.

pharmacokinetic studies of the hydrochloride salt of **8** (**8·HCl**) confirmed that the bioavailability was improved to 47%, and the good result of in vivo evaluation represented that **8** was a promising lead compound for development as an orally anticancer agent.

CHEMISTRY

The general steps to synthesize the target molecules have been outlined in Scheme 1. As we previously reported,[15] **3** reacted with 3-chloro-3-methyl-1-butyne, and the resulting compound was cyclized by heating in pyridine at 120 °C overnight and we got the key intermediate **5**. Subsequently, by Claisen–Schmidt condensation of **5** and aldehyde **6**, we got **7**, and then treating with Fe powder and NH_4Cl in ethanol/water easily obtained **8**. Encouraging by the previous studies, we then introduced a series of substituents to the amino group to find more effective compounds. We synthesized a series of alkyl substituted (**9a**–**9g**), amide (**9h**–**9n**), and sulfonamide (**9o**–**9r**) substituted compounds by using the traditional ways, and we also introduced amino acid to the structure (**9s**–**9t**). Those compounds were evaluated for the antiproliferative activity in vitro, but the results were disappointing and the tactics couldn't improve the activity. Hence, we introduced the compound **8** to its hydrochloride salt to approve the bioavailability.

dx.doi.org/10.1021/jm500849z | J. Med. Chem. 2014, 57, 7977–7989

Table 1. In Vitro Cell Growth Inhibitory Effects of 8, 9a−9t, and Millepachine

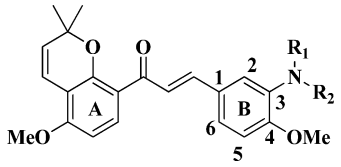

compd	R_1	R_2	$IC_{50} \pm SEM^a$, nM		
			HepG2	A375	K562
8	H	H	8 ± 1	22 ± 1	18 ± 2
9a	H	Me	>2000	>2000	>2000
9b	H		1640 ± 180	1600 ± 170	1580 ± 148
9c	H	Bn	970 ± 44	790 ± 52	1856 ± 116
9d	H	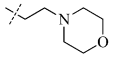	>2000	>2000	>2000
9e	Bn	Bn	>2000	>2000	114 ± 10
9f	Et	Et	>2000	>2000	>2000
9g			>2000	>2000	1500 ± 114
9h	H	Ac	570 ± 48	430 ± 60	700 ±90
9i	H		910 ± 96	920 ± 78	800 ± 48
9j	H		840 ± 74	1120 ± 96	1120 ± 84
9k	H	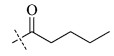	1300 ± 210	1590 ± 150	1160 ± 44
9l	H		830 ± 78	530 ± 26	570 ± 30
9m	H		1640 ± 96	1990 ± 48	1540 ± 222
9n	H	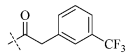	>2000	>2000	>2000
9o	H		2000 ± 290	1800 ± 240	1770 ± 268
9p	H		1960 ± 110	1870 ± 130	1580 ± 40
9q	H	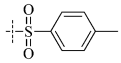	>2000	>2000	>2000
9r	H	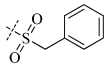	>2000	2000	>2000
9s	H	Gly	280 ± 30	700 ± 90	890 ± 50
9t	H	*D*-Ala	110 ± 30	360 ± 60	220 ± 22
millepachine (1)			1510 ± 120	3580 ± 320	4560 ± 320
colchicine			42 ± 11	12 ± 3	16 ± 5

[a] IC_{50} = compound concentration required to inhibit tumor cell proliferation by 50%. Data are expressed as the mean ± SEM from the dose−response curves of at least three independent experiments.

BIOLOGICAL RESULTS AND DISCUSSION

In Vitro Antiproliferative Activities. The synthesized derivatives **8** and **9a−9t** were evaluated for their antiproliferative activity against HepG2 cells, A375 cells, and K562 cells using MTT assay. Millepachine (**1**) and colchicine were used as the reference compounds. As shown in Table 1, the addition of amino group at the C-3 position on the B-ring of millepachine to furnish derivative **8** caused a significant increase of antiproliferative activity. Compared with millepachine, **8** showed nanomolar antiproliferative activity (IC_{50} = 8, 22, and 18 nM against HepG2, A375, and K562 cells, respectively) and resulted in a 163−253-fold increase in potency. Introductions of substituted amino groups, **9a−9g**, caused significant loss of the antiproliferative activities in contrasted to **1**. Then we introduced a series of amide, **9h−9l**. With the increase of the length of the alkyl chain of the amide, there was a significant decrease in antiproliferative activity. Compound **9m** with a guanidine structure at the C-3 position showed a reduction in antiproliferative activity compared with **1** on HepG2 cells. At the same time, the antiproliferative activities of the sulfonamide derivatives (**9o−9r**) were similar to **1**, and their IC_{50}s were more than 2 μM. In addition, the amino acid derivatives **9s** and **9t** were more potent than millepachine but still showed lower activity than compound **8**. The results indicated that the amino group was the key structure to keep the antiproliferative activity.

Then we focused on the evaluation of the antiproliferative activity of **8** across various tumor cells, with taxol and colchicine as the positive controls. As summarized in Table 2, the tumor cells were evaluated including cancer cell lines coming from colon, lung, liver, breast, and ovarian cancers. Similar to taxol and colchicine, **8** possessed potent inhibitory activity, with IC_{50}

dx.doi.org/10.1021/jm500849z | J. Med. Chem. 2014, 57, 7977−7989

Table 2. Activity of Selected Compound against Various Human Tumor Cell Lines

		$IC_{50} \pm SEM^a$ (nM)		
tumor type	cell line	**8**	taxol	colchicine
colon	C26	26 ± 2	210 ± 24	344 ± 36
	HCT116	21 ± 1	18 ± 2	15 ± 1
	DLD-1	18 ± 11	16 ± 2	11 ± 3
	HCT-15	19 ± 3	24 ± 4	16 ± 5
lung	NCI-H358	12 ± 5	2 ± 1	4 ± 1
liver	HepG2	8 ± 1	38 ± 9	42 ± 11
breast	MCF-7	27 ± 4	132 ± 21	58 ± 13
ovarian	ES-2	8 ± 5	20 ± 12	18 ± 9
	A2780S	20 ± 4	4 ± 2	4 ± 1
stomach	AGS	10 ± 2	8 ± 3	9 ± 1
glioma	U251	24 ± 5	23 ± 7	20 ± 9

[a]IC_{50} = compound concentration required to inhibit tumor cell proliferation by 50%. Data are expressed as the mean ± SEM from the dose−response curves of at least three independent experiments.

values ranged from 8 to 27 nM against all the tested tumor cell lines. It was worth noting that **8** was more potent than taxol and colchicine against C26, MCF-7, HepG2, and ES-2 cells.

Effect of 8 on Multidrug Resistant Cells. Drug resistance has become a critical problem for the first-line chemotherapy.[16,17] The common mechanisms of resistance identified in preclinical or clinical study include the overexpression of a cellular membrane protein called P-glycoprotein (P-gp) or changing in the levels of expression of different β-tubulin isotypes (β-III gene).[16−19] For example, cisplatin resistant human ovarian cancer cell line A2780CP, adriamycin resistant human breast carcinoma cell line MCF-7/ADR, and taxol resistant human colon cancer cell line HCT-8/T are all P-gp overexpressed, and taxol resistant human ovarian cancer cell lines A2780/T are β-tubulin III overexpressed. Hence, we compared the activity of **8** for these resistant and their related sensitive cancer cells. As shown in Table 3, **8** exhibit potent cytotoxic active toward sensitive cells and resistant cells, the IC_{50} values of **8** against A2780/T, A2780CP, MCF-7/ADR, and HCT-8/T cell lines were 84, 14, 17, and 152 nM, respectively. Compared with taxol, cisplatin, and adriamycin, **8** had much lower resistance indexes (4.2 for A2780/T, 0.7 for A2780CP, 1.6 for MCF-7/ADR, and 9.5 for HCT-8/T) than taxol (26.8 for A2780/T and 53.2 for HCT-8/T), adriamycin (240.9 for MCF-7/ADR), and cisplatin (8.6 for A2780CP). These results suggested that the P-gp and β-tubulin III gene might have no influence on the antiproliferative activity of **8**, suggesting that **8** might be useful in the treatment of drug refractory tumors, especially those with resistance to other antitubulin drugs.

Cell Cycle Effects and Induced Apoptosis. To explore whether the cytotoxicity of **8** was due to the cell cycle arrest, we examined the effect on cell cycle progression using propidium iodide (PI) staining by flow cytometry analysis in HepG2 cells. As shown in Figure 1A,C, **8** caused a significantly G2/M arrest in a concentration-dependent manner. The percentage of G2/M peak increased from 11.2% (control) to 19.5% at 50 nM of **8**, while at higher concentrations, more than 43.3% of the cells were arrested in G2/M after 24 h treatment.

Table 3. In Vitro Cell Growth Inhibitory Effects of 8 on Drug Resistant Cell Lines

	$IC_{50} \pm SEM^a$ (nM)		
compd	A2780S	A2780/T	resistance ratio[b]
8	20 ± 4	84 ± 34	4.2
taxol	4 ± 2	107 ± 12	26.8
	$IC_{50} \pm SEM^a$ (nM)		
compd	A2780S	A2780CP	resistance ratio[b]
8	20 ± 4	14 ± 2	0.7
cisplatin	1560 ± 140	13400 ± 370	8.6
	$IC_{50} \pm SEM^a$ (nM)		
compd	MCF-7	MCF-7/ADR	resistance ratio[b]
8	27 ± 4	17 ± 2	1.6
adriamycin	22 ± 8	5300 ± 400	240.9
	$IC_{50} \pm SEM^a$ (nM)		
compd	HCT-8	HCT-8/T	resistance ratio[b]
8	16 ± 3	152 ± 27	9.5
taxol	5 ± 1	266 ± 38	53.2

[a]IC_{50} = compound concentration required to inhibit tumor cell proliferation by 50%. Data are expressed as the mean ± SEM from the dose−response curves of at least three independent experiments. [b]The values express the ratio between IC_{50} determined in resistant and nonresistant cell lines.

Next, we evaluated the ability of **8** to induce cell death by a biparametric cytofluorimetric analysis using fluorescent immunolabeling of the protein annexin-V(V-FITC) and propidium iodide (PI). Dual staining for annexin-V and with PI can provide discrimination between live cells (annexin-V^-/PI^-), early apoptotic cells (annexin-V^+/PI^-), late apoptotic cells (annexin-V^+/PI^+), and necrotic cells (annexin-V^-/PI^+). As depicted in Figure 1B,D), treatment with **8** for 24 h induced an accumulation of early (annexin-V^+/PI^-) and late apoptotic cells (annexin-V^+/PI^+) in comparison with control in a concentration-dependent manner. The percentages of annexin-V positive cells were then further increased at 48 h.

Analysis of Immunofluorescence Staining. Given that the biological activity of chalcones has been reported to be bound up with tubulin,[12,13,15,20] to investigate whether the antiproliferative activities of **8** was derived from an interaction with tubulin, we examined the effect on the cellular microtubule network treated with compound **8** for 24 h and stained for DNA (blue) and α-tubulin (green). As shown in Figure 2, the microtubule network in HepG2 cells exhibited normal arrangement and organization in the absence of drug treatment. In contrast, after exposure to 1 μM **8** for 24 h, the microtubule polymerization and spindle formation showed distinct abnormalities, and HepG2 cells became arrested in mitosis and the mitotic cells had abnormal mitotic spindles. The mitotic cells acquired multiple tubulin bundles (multipolar) without chromosomes aligned at the metaphase plate with more dispersion of the chromosomes, suggesting that tubulin might be an effective target for **8**.

Effects on Microtubule Dynamics. It is well-known that the tubulin binding agents were divided into two types: stabilizing agents (e.g., taxol) and polymerization inhibitors (e.g., colchicine and CA-4).[7−9] To confirm which type the compound **8** related to, **8** was employed at 0.5, 2, and 5 μM, respectively, for microtubule dynamics assays. As shown in Figure 3, **8** inhibited tubulin polymerization in a concentration-dependent manner and the activity was higher than the positive colchicine at the same concentration. These data indicated that

dx.doi.org/10.1021/jm500849z | J. Med. Chem. 2014, 57, 7977−7989

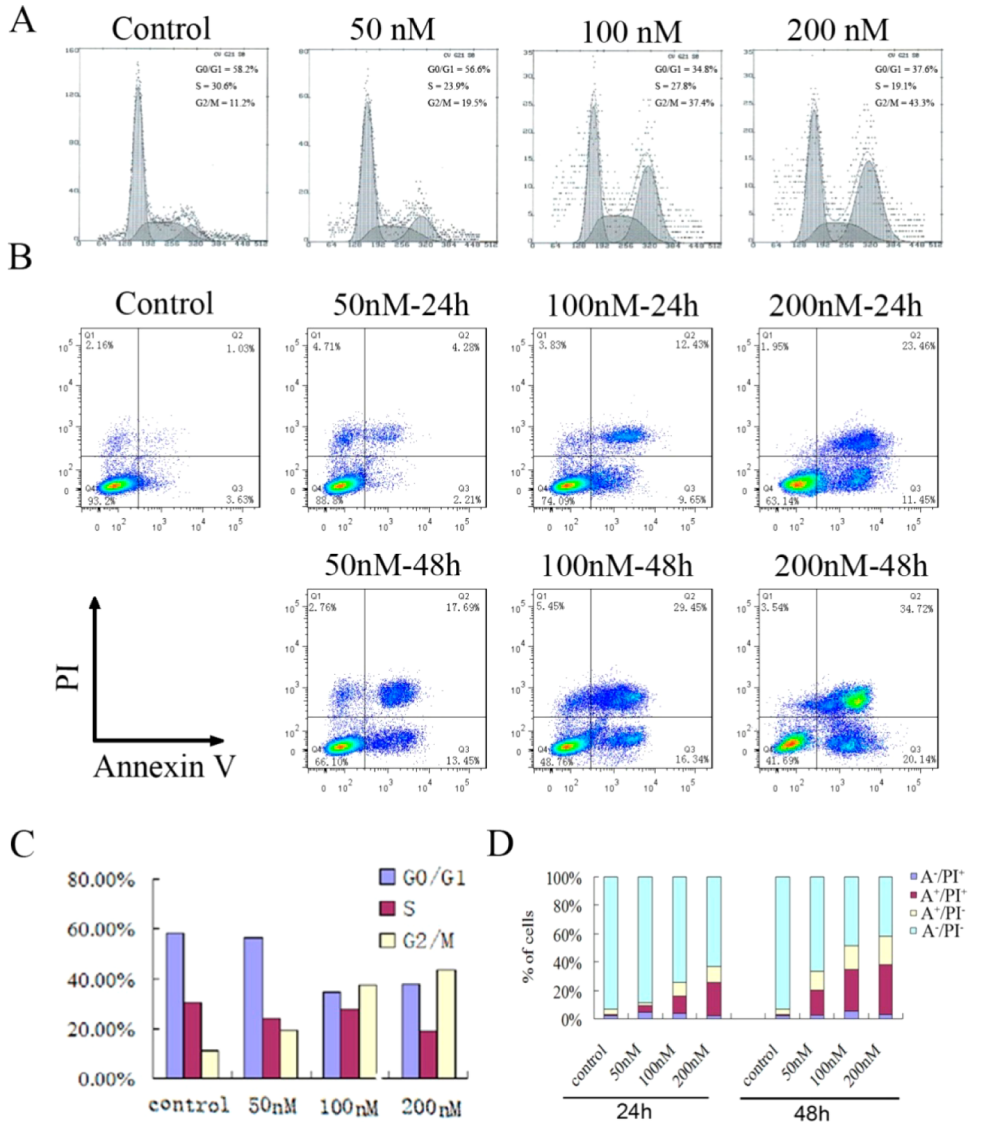

Figure 1. (A) Effects of **8** on cell cycle phase arrest in HepG2 cells. Cells were treated with 50, 100, and 200 nM of **8** for 24 h. Then the cells were fixed and stained with PI to analyze DNA content by flow cytometry. (B) representative flow cytometric histograms of apoptotic HepG2 cells after 24 or 48 h treatment with **8**. The cells were harvested and labeled with annexin-V-FITC and PI and analyzed by flow cytometry. (C) Percentages of cells in the different phases of the cell cycle. (D) Percentage of cells found in the different regions of the biparametric histograms after incubation with **8** for 24 or 48 h as indicated.

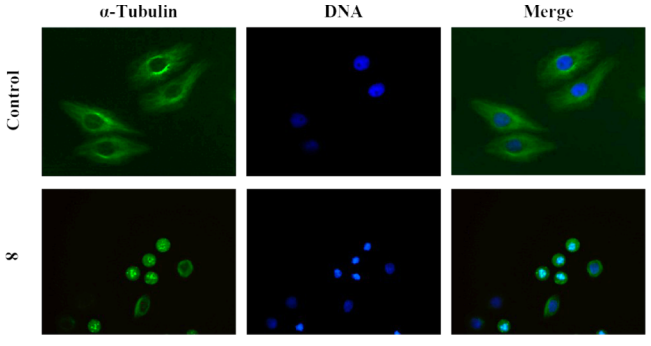

Figure 2. Effects of **8** on the microtubule network of HepG2 cells. Untreated (control) and cells treated with compound **8** at concentration of 1 μM for 24 h were fixed in methanol and stained with α-tubulin and counterstained with 4,6-diamidino-2-phenylindole (DAPI). Microtubules and unassembled tubulin are shown in green. DNA, stained with DAPI, is shown in blue.

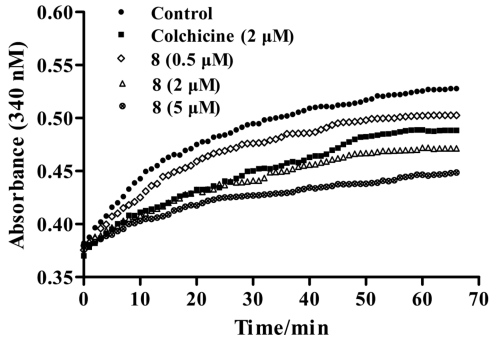

Figure 3. Effect of **8** on tubulin polymerization. Tubulin had been preincubated for 5 min with **8** at 0.5, 2, and 5 μM, at 2 μM and vehicle DMSO at room temperature before GTP was added to start the tubulin polymerization reactions. The reaction was monitored at OD340 nm at 37 °C.

dx.doi.org/10.1021/jm500849z | J. Med. Chem. 2014, 57, 7977−7989

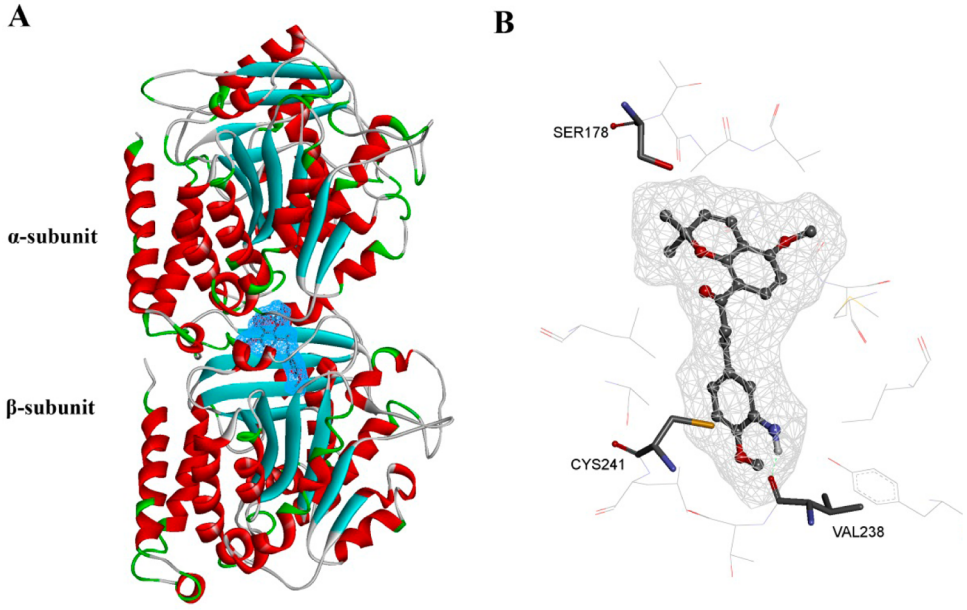

Figure 4. (A) Overview of the binding modes of **8** in tubulin crystal structure 3HKD. (B) Close view of the potential binding pose of **8** in 3HKD.

the mechanism was different from our previously reported compound **2**, which was a microtubule stabilizing agent binding to the taxol site.[12] Our results demonstrating that compound **8** might bind to the colchicine site as a novel tubulin polymerization inhibitor agent.

Molecular Modeling. To rationalize our experimental findings, a series of molecular docking simulations on tubulin were performed using a procedure reported previously.[12−15] Interestingly, **8** showed the best docking score in 3HKD. The overview of the binding site of **8** is shown in Figure 4A. This binding pocket is located on the interface between the α- and β-subunits of the tubulin dimer and extended slightly out of the β-subunit. The B-ring of **8** went deep into the pocket, and the amino group at C-3 position provided a potential hydrogen bond interaction with the VAL238 (Figure 4B). This hydrogen bond stabilized the interaction of **8** with the binding pocket, and this may explain why little tolerance is allowed for substituted amino groups.[20,21]

Pharmacokinetic Studies. It was known that most of chalcones have the problems of low aqueous solubility and bioavailability which limited the administration of these compounds.[21,22] There are many well-known formulation techniques to increase aqueous solubility, e.g., micronization, nanosizing, or complexation with cyclodextrins, and formation of salts is a well-known technique to modify and optimize the solubility and dissolution rate properties of an ionizable research.[23] Hence, a series of salts based on compound **8** were synthesized according to the literature[24] and evaluated the solubility and pH values. As shown in Table 4, the solubility in aqueous buffer indeed had a significant improvement, especially the hydrochloride salt **8·HCl** and sulfate salt **8·H_2SO_4**, their solubility were up to 64 and 58 μg/mL, respectively. Considering the pH values, we chose the **8·HCl** and **8·H_2SO_4** to evaluate their acute toxicity information by short-duration dose-ranging studies that defined as maximum tolerated dose (MTD), which was used to determine the largest dose possible before one death occurs in the test animals, and the result was presented in Table 5; the **8·HCl** had the higher MTD value compared with **8·H_2SO_4**, and the

Table 4. Antiproliferative Activity on HepG2 Cell, Aqueous Solubility, and pH of Several Kinds of Salts

compd	IC_{50} ± SEM[a] (nM)	solubility (μg/mL)[b]	pH[c]
8	8 ± 1	8	7.3
hydrochloride salt (**8·HCl**)	9 ± 1	64	3.5
sulfate salt (**8·H_2SO_4**)	11 ± 2	58	2.5
mesylate salt (**8·$MeSO_2H$**)	10 ± 1	50	2.8
maleate salt (**8·maleate**)	12 ± 3	47	5
tartrate salt (**8·tartrate**)	11 ± 3	52	4

[a]IC_{50} = compound concentration required to inhibit tumor cell proliferation by 50%. [b]Maximum soluble concentration in PBS determined by nephelometry. [c]Measured by pH electrode.

Table 5. Acute Toxicity of 8·HCl, 8·H_2SO_4, and Taxol on BALB/c Mice

parameters	8·HCl	8·H_2SO_4	taxol
MTD[a] (mg/kg)	250	200	30

[a]MTD, the maximum tolerated dose.

MTD of **8·HCl** was 250 mg/kg in comparsion with 30 mg/kg of taxol.[25]

The pharmacokinetic studies of **8** were compared with **8·HCl**. As shown in Table 6, the bioavailability of compound **8** was 28%, while the hydrochloride **8·HCl** had shown a significant increase, which was up to 47%. The result suggested that **8**, especially its hydrochloride salt **8·HCl**, may be developed as an orally bioavailable anticancer agent.

In Vitro Evaluation of Antivascular Activity of 8. Most microtubule binding drugs possess vascular disrupting activity, which are thought to disrupt microtubule dynamics to induce endothelial cell shape change. We used HUVEC cells culture assay to test the ability of **8** to induce rapid endothelial cell shape changes. As the migration of ECs is the key step to generate new blood vessels, wound-healing migration assay was applied to assess the HUVECs migration. As shown in Figure 5A, the untreated cells migrated to fill the area that was initially scraped after 24 h, in contrast, compound **8** significantly inhibited the

dx.doi.org/10.1021/jm500849z | J. Med. Chem. 2014, 57, 7977−7989

Table 6. Pharmacokinetic Parameters Tested in Vivo

	8		8·HCl	
route	iv	po	iv	po
N^a	5	5	5	4
dose (mg/kg)	2.25	9	3	15
CL (L/h/kg)^b	1.2 ± 0.3	5.9 ± 4	3.0 ± 0.5	7.4 ± 3
V_{ss} (L/kg)^c	21 ± 22	25 ± 30	31 ± 21	47 ± 35
AUC (μg/mL·h)^d	1807 ± 355	2043 ± 970	973 ± 170	2264 ± 1334
C_{max} (μg/mL)^e	2938 ± 586	519 ± 480	1506 ± 273	449 ± 74
F (%)^f	28		47	

^{a}Numbers of rats. ^{b}Systemic clearance. ^{c}Volume of distribution following intravenous dosing. ^{d}Area under the curve following intravenous dosing, integrated drug concentration with respect to time and integrated drug concentration with respect to time following oral dosing. ^{e}Maximum plasma concentration following intravenous dosing. ^{f}Percent oral bioavailability.

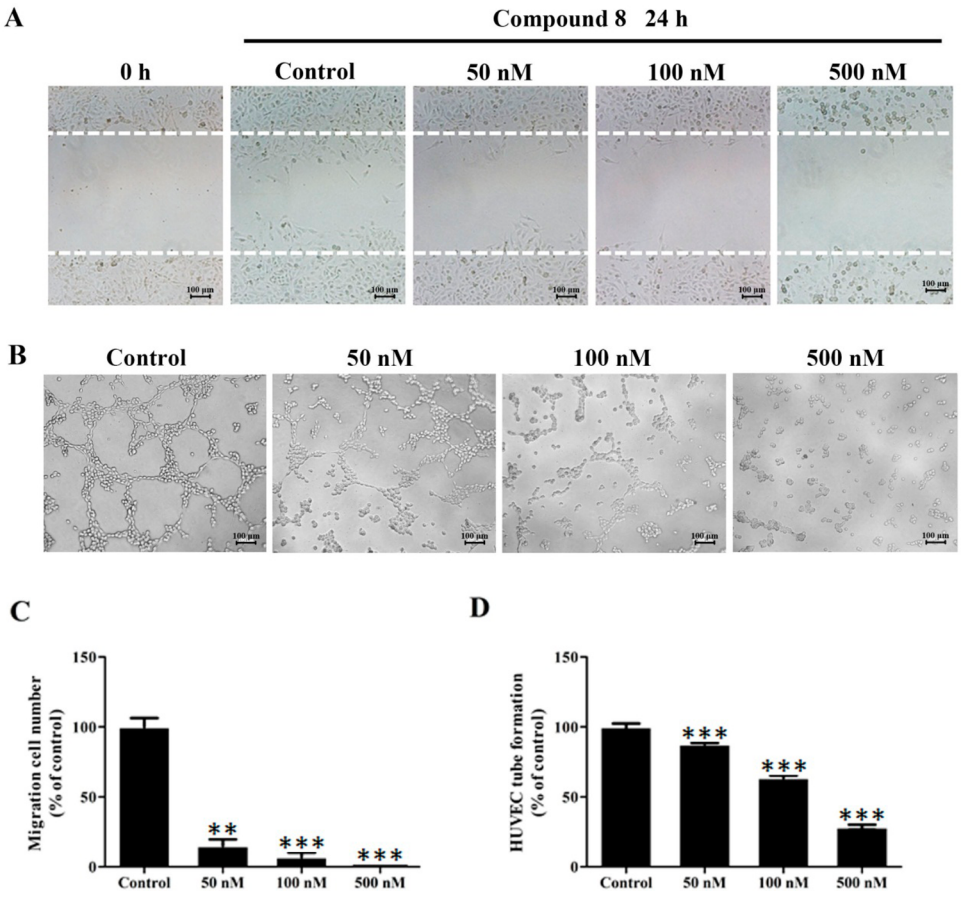

Figure 5. Effects on the HUVECs migration and tube formation. (A) HUVECs suspended in serum-free Dulbecco's Modified Eagle Medium (DMEM) containing **8** (50, 100, and 500 nM) for 20 h were photographed under a phase contrast microscopy (magnification: 100). Control was treated with serum-free DMEM. (B) HUVECs (1×10^4 cells) suspended in DMEM containing **8** (50, 100, and 500 nM) were added to the Matrigel. Control was treated with DMEM alone. After incubation for 6 h at 37 °C, capillary networks were photographed and quantified (magnification: 100×). (C) Statistical data of cell migration assay. (D) Statistical data of tube formation assay. **, $P < 0.01$; ***, $P < 0.001$, significantly different compared with control by *t*-test.

HUVEC migration in a concentration-dependent manner (Figures 5B,C).

Then we also evaluated the ability of compound **8** in a tube formation assay. After being seeded on Matrigel, HUVECs form a capillary-like tubules with multicentric junctions. After 6 h treatment in different concentrations (50−500 nM) of compound **8**, the capillary-like tubes were interrupted in different levels. At the two higher concentrations of **8**, most cells were spherical and aggregated in small clumps (Figure 5B). Quantitative image analysis showed that **8** markedly decreased the capillary-like tubes in a concentration-dependent manner (Figure 5D).

To evalute if the inhibition of cell migration and tube formation was due to a cytotoxic action of **8**, we analyzed cell proliferation of the HUVECs by the MTT assay to determine the IC_{50} value of compound **8** at 48 h. The calculated IC_{50} of compound **8** was 0.45 ± 0.06 μM, which is higher than the concentration of 50 nM required for the inhibition of cell migration and tube formation. This result indicates that the

dx.doi.org/10.1021/jm500849z | J. Med. Chem. 2014, 57, 7977−7989

Table 7. Summary of Tumor Growth Inhibition

		administration			toxicity		antitumor activity
tumor model	compd	dose (mg/kg)	schedule[a]	route	body weight change (%)	death	tumor mass change (%)
C26	**8·HCl**	10	Q2D × 8	iv	+0.8	0/6	86
	taxol	5	Q4D × 4	iv	−3.7	0/6	76
A2780S	**8·HCl**	10	Q2D × 8	iv	−2.5	0/6	61
	cisplatin	5	Q4D × 4	ip	−31.9	2/6	60
A2780CP	**8·HCl**	10	Q2D × 7	iv	+1.0	0/6	51
	cisplatin	5	Q4D × 4	ip	−30.5	4/6	
	taxol	5	Q4D × 4	iv	−5.6	0/6	69
HepG2	**8·HCl**	25	Q2D × 11	po	+7.6	0/6	78
	adriamycin	5	Q2D × 11	iv	+0.5	0/6	61

[a]Q2D, every 2 days; Q4D, every 4 days; Q5D, every 5 days.

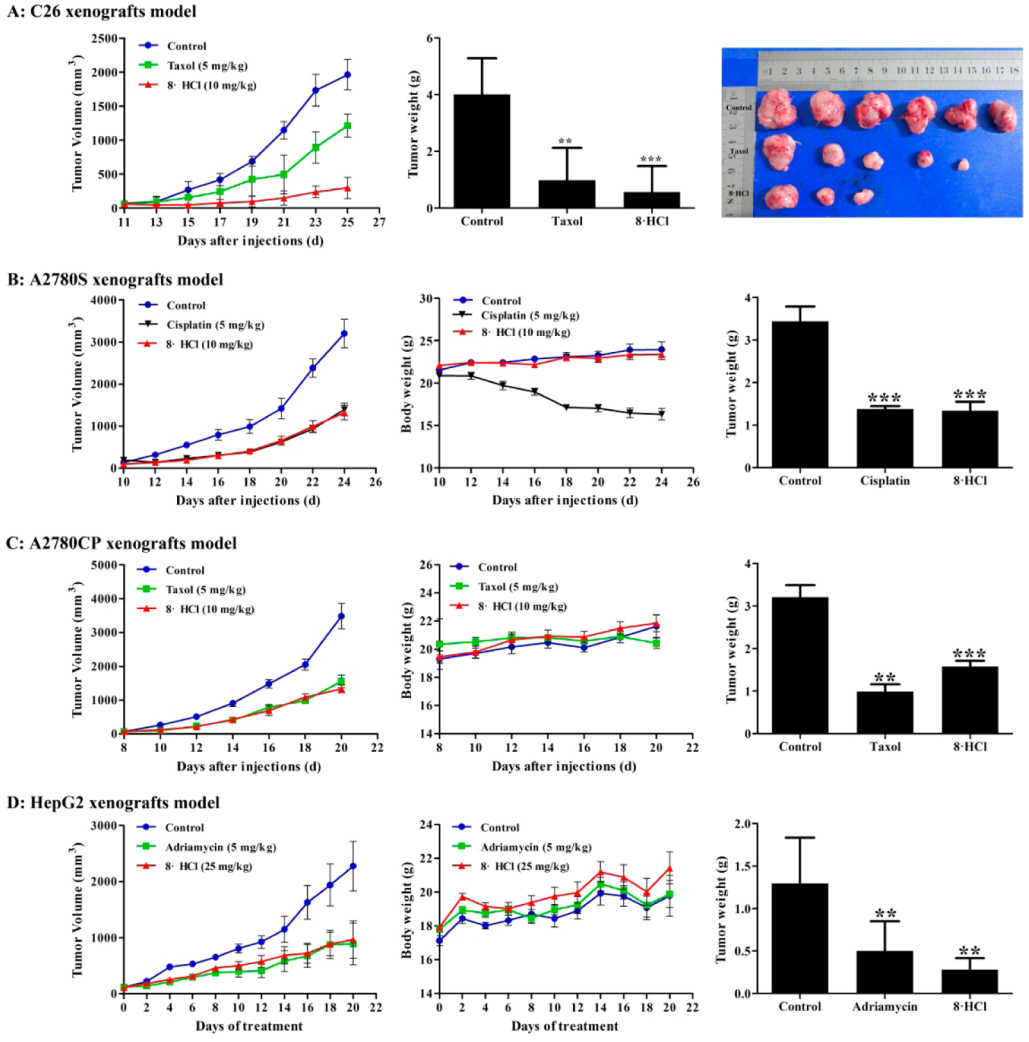

Figure 6. Effect of **8·HCl** inhibit the xenograft model growth. (A) **8·HCl** inhibited tumor growth on the C26 xenograft model. (B) **8·HCl** inhibited tumor growth on the A2780S xenograft model. (C) **8·HCl** inhibited tumor growth on the A2780CP xenograft model. (D) **8·HCl** inhibited tumor growth on the HepG2 xenograft model. **, $P < 0.01$; ***, $P < 0.001$, significantly different compared with control by *t*-test.

activity of **8** on HUVECs cell migration and tube formation is not due to a cytotoxic action at indicated concentration.

Antitumor Activity in Vivo. We established four xenograft models using a mice colon cancer line (C26), a couple of ovarian cancer (A2780S, A2780CP) lines, and a liver cancer line (HepG2) to investigate the effect of **8·HCl** on tumor growth. C26, A2780S, A2780CP, and HepG2 tumors were established by respective sc injection of 5×10^6 cells in the right armpit of the mice. Once the tumor volume reached a size of 100 mm^3, the mice were selected and randomized into treatment groups (6

dx.doi.org/10.1021/jm500849z | J. Med. Chem. 2014, 57, 7977−7989

mice per group). The administration, dosing schedules of **8·HCl** and results were presented in Table 7.

As displayed in Table 7, **8·HCl** showed remarkable reduction of tumor growth in all four xenograft tumor models. In C26 tumor model, treatment with 10 mg/kg iv administration of **8·HCl** caused a significantly suppression of tumor growth (Figure 6), three out of **8·HCl**-treated mice caused completely tumor reduction, and the average inhibitory rate reached 86% by the end of observation, while treatment with 5 mg/kg iv taxol caused 76% tumor reduction. The similar results were also observed in a pair of drug sensitive and resistant A2780S and A2780CP xenografts model. The inhibition rates were respectively 61% on an A2780S xenograft nude mice model and 51% on an A2780CP xenograft nude mice model. Compared with the control vehicle-treated mice, **8·HCl** did not cause obvious body weight loss, whereas significant weight loss were observed in the cisplatin groups. In the A2780S xenograft model, cisplatin-treated groups caused −31.9% body weight change and 2/6 death of mice due to the excessive body wight loss, while **8·HCl**-treated groups only caused −2.5% body weight change. The similar results were observed in the A2780CP xenograft model. In the A2780CP xenograft model, cisplatin-treated groups caused −30.5% body weight change and 4/6 death of mice, while **8·HCl** -treated groups did not cause body weight change at 10 mg/kg iv injection. These results proved that **8·HCl** were effective both in the drug sensitive and drug resistant tumors without obvious toxicity. As the bioavailability of **8·HCl** was up to 47%, it is possible to investigate the antitumor effect of oral administation of **8·HCl**. Hence, we also established a HepG2 xenografts model by oral administration of **8·HCl**. As shown in Table 7, treatment with oral administration of 25 mg/kg **8·HCl** every 2 days caused the significant reduction of tumor growth, and the inhibitory rate was up to 78% in comparison with 61% of adrimycin-treated group.

CONCLUSIONS

In summary, as a continued modification of millepachine, we have synthesized a series of novel derivatives and found that introduction of an amino group to the C-3 position on the B ring of millepachine led to a consistent increase in antiproliferative activity. Thus, **8** showed a 163−253-fold improvement of IC_{50} values on three cancer cell lines (HepG2, A375, and K562) in contrast to millepachine, and IC_{50} values ranged from 8 to 26 nM in the panel of tumor cell lines. Preliminary mode of action studies demonstrated that **8** caused accumulation of cells in the G2/M phase of the cell cycle and induced apoptosis in HepG2 cells. The antimitotic ability on multidrug resistant cells was also tested. The results demonstrated that **8** was not a substrate for P-glycoprotein drug pump or not affected by the β-tubulin III gene. Interestingly, the immunofluorescence assays, microtubule dynamics experiment, and molecular modeling studies identified that compound **8** was a polymerization inhibitor binding at the colchicine site. To improve the solubility and bioavailability, the compound **8** was formulated as its hydrochloride salt (**8·HCl**), and the pharmacokinetic studies showed that the **8·HCl** improved the bioavailability up to 47%. Then we evaluated the activity in vivo on four kinds of tumor models, and **8·HCl** was proved to have a potent effect on inhibiting the tumor growth without significant body weight loss or behavior disorders. Therefore, **8** as a tubulin polymerization inhibitor may be a potent anticancer agent.

EXPERIMENTAL SECTION

Chemistry. All the chemical solvents and reagents, which were analytically pure without further purification, were commercially available. TLC was performed on 0.20 mm Silica Gel 60 F_{254} plates (Qingdao Haiyang Chemical, China). ^{1}H NMR and ^{13}C NMR spectra were recorded on a Bruker Avance400 spectrometer (Bruker Company, Germany) or Varian spectrometer (Varian, Palo Alto, CA), using TMS as an internal standard. Chemical shifts were given in ppm (parts per million). Mass spectra were recorded on Q-TOF Priemier mass spectrometer (Micromass, Manchester, UK). The purity of each compound (>95%) was determined on an Waters e2695 series LC system (column, Xtimate C18, 4.6 mm × 150 mm, 5 μm; mobile phase, methanol (60%)/H_2O (40%); low rate, 1.0 mL/min; UV wavelength, 254−400 nm; temperature, 25 °C; injection volume, 10 μL).

*1-(4-Methoxy-2-((2-methylbut-3-yn-2-yl)oxy)phenyl) ethanone (**4**).* To a solution of **3** (1.66 g, 10 mmol) in CH_3CN (100 mL) was added DBU (1.5 mL, 15 mmol), $CuCl_2{\cdot}2H_2O$ (5 mg, 0.3 mol %), and 3-chloro-3-methyl-1-butyne (1.53 g, 15 mmol) at 0 °C. Then the mixture was stirred 5 h and monitored by TLC. After completed, 1 N HCl (aq) was added to adjust pH = 2. Then the solvent was removed under reduced pressure, the residue was poured into water (50 mL), and the white precipitate was collected by filtration to obtain **2** (1.97 g, 85%). ^{1}H NMR ($CDCl_3$, 400 MHz) δ: 1.75 (s, 6H), 2.58 (s, 3H), 2.69 (s, 1H), 3.84 (s, 3H), 6.58 (dd, 1H, J = 8.8 Hz, 2.0 Hz), 7.19 (d,1H, J = 2.0 Hz), 7.75 (d,1H, J = 8.8 Hz). ^{13}C NMR ($CDCl_3$,100 MHz) δ: 29.6, 31.9, 31.9, 55.5, 73.1, 75.1, 85.3, 104.9, 107.4, 124.6, 132.1, 156.9, 163.3, 198.5. MS (ESI, m/z): 255.05 $[M + Na]^+$.

*1-(5-Methoxy-2,2-dimethyl-2H-chromen-8-yl)ethanone (**5**).* A suspension of **4** (2.32 g, 10 mmol) in pyridine (50 mL) was stirred at 120 °C for 12 h and monitored by TLC. After completion, the mixture concentrated under reduced pressure to give **5** as black oil, without further purification. ^{1}H NMR ($CDCl_3$, 400 MHz) δ: 1.49 (s, 6H), 2.62 (s, 3H), 3.87 (s, 3H), 5.61 (d, 1H, J = 10.0 Hz), 6.47 (d, 1H, J = 8.8 Hz), 6.66 (d, 1H, J = 10.0 Hz), 7.73 (d, 1H, J = 8.8 Hz). MS (ESI, m/z): 255.14 $[M + Na]^+$.

*(E)-1-(5-Methoxy-2,2-dimethyl-2H-chromen-8-yl)-3-(4-methoxy-3-nitrophenyl)prop-2-en-1-one (**7**).* A solution of 50% KOH (3 mL, aq) was added dropwise to a stirred solution of **3** (232 mg, 1.0 mmol) and aldehyde **4** (1.0 mmol) in methanol (10 mL) at 0 °C. The resulting mixture was stirred at room temperature for under 24 h. After the end of reaction, the mixture was poured into ice−water and neutralized with 2 N HCl. The precipitated was filtered, washed with water, dried, and crystallized from ethanol to afford a solid. ^{1}H NMR (400 MHz, DMSO-d_6) δ: 8.25 (d, J = 1.6 Hz, 1H), 8.01 (dd, J = 8.8, 1.7 Hz, 1H), 7.63 (d, J = 15.8 Hz, 1H), 7.56 (dd, J = 12.2, 10.2 Hz, 2H), 7.47 (d, J = 8.8 Hz, 1H), 6.71 (d, J = 8.9 Hz, 1H), 6.62 (d, J = 10.1 Hz, 1H), 5.79 (d, J = 10.0 Hz, 1H), 3.98 (s, 3H), 3.87 (s, 3H), 1.45 (s, 6H). ^{13}C NMR (100 MHz, DMSO-d_6) δ: 188.49, 158.01, 153.00, 152.83, 139.48, 138.44, 133.65, 131.13, 129.37, 127.59, 127.33, 124.40, 120.77, 115.91, 114.98, 109.80, 104.21, 76.88, 56.97, 55.98, 27.50. MS (ESI, m/z): 396.21 $[M + H]^+$.

*(E)-3-(3-Amino-4-methoxyphenyl)-1-(5-methoxy-2,2-dimethyl-2H-chromen-8-yl)prop-2-en-1-one (**8**).* To (*E*)-1-(5-Methoxy-2,2-dimethyl-2*H*-chromen-8-yl)-3-(4-methoxy-3-nitrophenyl)prop-2-en-1-one (792 mg, 2 mmol) (**7**) in EtOH (10 mL) and water (3 mL) was added iron powder (335 mg, 6.7 mmol) and NH_4Cl (64 mg, 1.2 mmol). The reaction was stirred at 85 °C for 1 h, cooled to room temperature, and filtered through Celite. The filter cake was washed with dichloromethane (20 mL), and the filtrate was concentrated under pressure. The residue was dissolved in dichloromethane (15 mL), washed with water (5 mL), dried over Na_2SO_4, filtered, and concentrated. The residue was purified by flash column chromatography to give the title compound **8** (yellow solid, 540 mg, 74%); mp 146−148 °C. ^{1}H NMR (400 MHz, DMSO-d_6) δ: 7.54 (d, J = 8.7 Hz, 1H), 7.40 (s, 2H), 6.95 (s, 1H), 6.93−6.84 (m, 2H), 6.70 (d, J = 8.8 Hz, 1H), 6.63 (d, J = 10.0 Hz, 1H), 5.80 (d, J = 10.0 Hz, 1H), 4.94 (s, 2H), 3.86 (s, 3H), 3.82 (s, 3H), 1.46 (s, 6H). ^{13}C NMR (100 MHz, DMSO-d_6) δ: 188.80, 157.64, 152.48, 148.69, 142.48, 138.11, 130.99, 129.38, 127.55, 123.84, 121.33, 118.47, 116.02, 111.71, 110.49, 109.80, 104.07, 76.68, 55.89, 55.37, 27.48. MS (ESI, m/z): 366.24 $[M + H]^+$. Compound **8·HCl**: ^{1}H NMR (400 MHz, DMSO-d_6) δ 7.62−7.42 (m, 5H), 7.21 (s, 1H), 6.72

dx.doi.org/10.1021/jm500849z | J. Med. Chem. 2014, 57, 7977−7989

(d, J = 8.6 Hz, 1H), 6.63 (d, J = 9.9 Hz, 1H), 5.80 (d, J = 10.0 Hz, 1H), 3.93 (s, 3H), 3.87 (s, 3H), 1.46 (s, 6H).

General Procedures of Method A for the Synthesis of 9a−9g. To a solution of compound **8** (365 mg, 1 mmol) in anhydrous CH_3CN (10 mL) was added anhydrous K_2CO_3 (0.345 g, 2.5 mmol). After stirred over 15 min at room temperature, RX (2 equiv) was added into the slurry. The reaction mixture was stirred at reflux for 6 h. The reaction mixture was filtrate and diluted with EtOAc, then washed by water and brine, dried over anhydrous Na_2SO_4, and concentrated in vacuo. The residue was purified by flash chromatograph using petroleum ether/ethyl acetate (5:1) as eluent to give the title compounds.

*(E)-1-(5-Methoxy-2,2-dimethyl-2H-chromen-8-yl)-3-(4-methoxy-3-(methylamino)phenyl)prop-2-en-1-one (**9a**).* **9a** was obtained from **8** and iodomethane as described for method A: 239 mg, 63% yield as a yellow solid; mp 103−105 °C. ^{1}H NMR (400 MHz, $CDCl_3$) δ: 7.72 (d, J = 8.8 Hz, 1H), 7.70−7.59 (m, 2H), 6.93 (d, J = 8.1 Hz, 1H), 6.87 (d, J = 6.0 Hz, 1H), 6.76 (d, J = 7.9 Hz, 1H), 6.70 (d, J = 10.0 Hz, 1H), 6.52 (d, J = 8.8 Hz, 1H), 5.63 (d, J = 10.0 Hz, 1H), 3.88 (s, 6H), 2.90 (s, 3H), 1.52 (s, 6H). ^{13}C NMR (100 MHz, DMSO-d_6) δ: 188.45, 157.74, 152.57, 148.91, 142.52, 139.61, 131.10, 129.22, 127.87, 123.83, 121.27, 118.72, 116.06, 109.79, 109.37, 105.35, 104.14, 76.69, 55.92, 55.46, 29.58, 27.49. MS (ESI, m/z): 380.21 $[M + H]^+$.

*(E)-1-(5-Methoxy-2,2-dimethyl-2H-chromen-8-yl)-3-(4-methoxy-3-(prop-2-yn-1-ylamino)phenyl)prop-2-en-1-one (**9b**).* **9b** was obtained from **8** and 3-bromopropyne as described for method A: 379 mg, 94% yield as a yellow solid; mp 138−140 °C. ^{1}H NMR (400 MHz, $CDCl_3$) δ: 7.71 (d, J = 8.8 Hz, 1H), 7.68 (d, J = 16 Hz, 1H), 7.60 (d, J = 16 Hz, 1H), 7.04 (d, J = 8.4 Hz, 1H), 7.00 (s, 1H), 6.81 (d, J = 8.1 Hz, 1H), 6.70 (d, J = 10.0 Hz, 1H), 6.52 (d, J = 8.8 Hz, 1H), 5.62 (d, J = 10.0 Hz, 1H), 4.01 (s, 2H), 3.89 (s, 3H), 3.88 (s, 3H), 2.22 (s, 1H), 1.53 (s, 6H). ^{13}C NMR (100 MHz, DMSO-d_6) δ: 188.75, 157.73, 152.52, 149.21, 142.68, 137.17, 131.08, 129.37, 127.51, 123.78, 121.24, 119.83, 115.98, 109.82, 109.78, 107.23, 104.16, 81.78, 76.76, 72.96, 55.92, 55.53, 31.68, 27.56. MS (ESI, m/z): 404.29 $[M + H]^+$.

*(E)-3-(3-(Benzylamino)-4-methoxyphenyl)-1-(5-methoxy-2,2-dimethyl-2H-chromen-8-yl)prop-2-en-1-one (**9c**) and (E)-3-(3-(Dibenzylamino)-4-methoxyphenyl)-1-(5-methoxy-2,2-dimethyl-2H-chromen-8-yl)prop-2-en-1-one (**9e**).* **9c** and **9e** was obtained from **8** and (bromomethyl)benzene as described for method A: **9c**, 159 mg, 35% yield as a yellow solid; mp 95−97 °C. ^{1}H NMR (400 MHz, $CDCl_3$) δ: 7.69 (d, J = 8.8 Hz, 1H), 7.62 (d, J = 15.7 Hz, 1H), 7.53 (d, J = 15.7 Hz, 1H), 7.36−7.27 (m, 5H), 6.96 (dd, J = 8.2, 1.7 Hz, 1H), 6.88 (d, J = 1.7 Hz, 1H), 6.79 (d, J = 8.2 Hz, 1H), 6.68 (d, J = 10.0 Hz, 1H), 6.50 (d, J = 8.8 Hz, 1H), 5.60 (d, J = 10.0 Hz, 1H), 4.37 (s, 2H), 3.89 (s, 3H), 3.87 (s, 3H), 1.45 (s, 6H). ^{13}C NMR (100 MHz, DMSO-d_6) δ: 157.63, 152.38, 148.79, 142.70, 139.81, 138.16, 130.97, 129.28, 128.31, 128.13, 127.59, 126.76, 126.62, 123.70, 121.28, 118.53, 115.99, 109.79, 109.73, 106.86, 104.11, 76.57, 55.92, 55.59, 45.86, 27.42. MS (ESI, m/z): 456.18 $[M + H]^+$. **9e**, 229 mg, 42% yield as a yellow solid; mp 108−110 °C. ^{1}H NMR (400 MHz, $CDCl_3$) δ: 7.67 (d, J = 8.6 Hz, 1H), 7.54 (d, J = 15.7 Hz, 1H), 7.45 (d, J = 15.7 Hz, 1H), 7.36 (d, J = 4.4 Hz, 1H), 7.28 (s, 2H), 7.27−7.16 (m, 9H), 7.06 (s, 1H), 6.91 (d, J = 8.4 Hz, 1H), 6.68 (d, J = 10.0 Hz, 1H), 6.49 (d, J = 8.9 Hz, 1H), 5.61 (d, J = 10.0 Hz, 1H), 4.25 (s, 3H), 3.96 (s, 3H), 3.87 (s, 4H), 1.43 (s, 6H). ^{13}C NMR (100 MHz, DMSO-d_6) δ: 188.61, 157.73, 154.95, 152.48, 141.81, 139.17, 138.42, 131.03, 129.25, 128.36, 128.12, 128.11, 127.04, 127.04, 126.83, 126.64, 124.17, 123.98, 121.16, 120.37, 115.98, 112.23, 109.74, 104.13, 76.67, 55.92, 55.76, 54.85, 54.86, 27.52. MS (ESI, m/z): 546.36 $[M + H]^+$.

*(E)-1-(5-Methoxy-2,2-dimethyl-2H-chromen-8-yl)-3-(4-methoxy-3-((2-morpholinoethyl)amino)phenyl)prop-2-en-1-one (**9d**).* **9d** was obtained from **8** and 4-(2-chloroethyl)morpholine as described for method A: 416 mg, 87% yield as a yellow solid; mp 113−115 °C. ^{1}H NMR (400 MHz, $CDCl_3$) δ: 7.71 (d, J = 8.8 Hz, 1H), 7.65 (d, J = 15.7 Hz, 1H), 7.58 (d, J = 15.7 Hz, 1H), 6.96 (d, J = 7.9 Hz, 1H), 6.86 (s, 1H), 6.77 (d, J = 8.2 Hz, 1H), 6.70 (d, J = 10.0 Hz, 1H), 6.52 (d, J = 8.8 Hz, 1H), 5.63 (d, J = 10.0 Hz, 1H), 4.82 (s, 1H), 3.91 (s, 3H), 3.89 (s, 3H), 3.73 (s, 4H), 3.21 (s, 2H), 2.70 (s, 2H), 2.49 (s, 4H), 1.51 (s, 6H). ^{13}C NMR (100 MHz, DMSO-d_6) δ: 189.20, 157.56, 152.41, 148.98, 142.62, 137.14, 130.87, 129.35, 127.90, 124.44, 121.40, 118.20, 115.98, 110.20, 109.75, 108.80, 104.02, 76.66, 63.07, 55.94, 55.59, 54.41, 51.08, 37.11, 27.60. MS (ESI, m/z): 479.28 $[M + H]^+$.

*(E)-3-(3-(Diethylamino)-4-methoxyphenyl)-1-(5-methoxy-2,2-dimethyl-2H-chromen-8-yl)prop-2-en-1-one (**9f**).* **9f** was obtained from **8** and 4-(2-chloroethyl)morpholine as described for method A: 387 mg, 92% yield as a yellow solid; mp 107−109 °C. ^{1}H NMR (400 MHz, $CDCl_3$) δ: 7.71 (d, J = 8.8 Hz, 1H), 7.66 (d, J = 15.6 Hz, 1H), 7.59 (d, J = 15.6 Hz, 1H), 7.24 (d, J = 7.3 Hz, 1H), 6.90 (dd, J = 19.7, 6.8 Hz, 2H), 6.76 (d, J = 8.1 Hz, 1H), 6.70 (d, J = 10.0 Hz, 1H), 6.52 (d, J = 8.8 Hz, 1H), 5.63 (d, J = 10.0 Hz, 1H), 3.89 (d, J = 7.2 Hz, 6H), 3.19 (q, J = 6.7 Hz, 4H), 1.51 (s, 6H), 1.31 (t, J = 7.1 Hz, 2H), 1.04 (t, J = 7.0 Hz, 3H). MS (ESI, m/z): 422.13 $[M + H]^+$.

*(E)-3-(3-(Bis(3-methylbut-2-en-1-yl)amino)-4-methoxyphenyl)-1-(5-methoxy-2,2-dimethyl-2H-chromen-8-yl)prop-2-en-1-one (**9g**).* **9g** was obtained from **8** and 1-bromo-3-methylbut-2-ene as described for method A: 440 mg, 88% yield as a yellow solid; mp 87−89 °C. ^{1}H NMR ($CDCl_3$, 400 MHz) δ: 1.50 (s, 6H), 1.61 (s, 6H), 1.74(m, 6H), 3.87 (s, 3H), 3.89 (s, 3H), 4.59 (d, 4H, J = 6.4 Hz), 5.53 (m, 1H), 5.62 (d,1H, J = 10.0 Hz), 6.50 (d,1H, J = 8.8 Hz), 6.68 (d, 1H, J = 9.6 Hz), 6.85−6.88 (m, 2H), 7.14−7.17(m, 2H), 7.56 (d, 1H, J = 16.0 Hz), 7.62 (d, 1H, J = 16.0 Hz), 7.70 (d, 1H, J = 8.8 Hz). MS (ESI, m/z): 502.13 $[M + H]^+$.

General Procedures of Method B for the Synthesis of 9h−9k and 9n. RCOOH (1.5 mmol) was added to a stirred mixture of compound **8** (365 mg, 1 mmol), EDCI (288 mg, 1.5 mmol), and DMAP (61 mg, 0.5 mmol) in anhydrous CH_2Cl_2 (5 mL). The mixture was stirred at room temperature for 12 h. On completion, the slurry was partitioned between water (20 mL) and CH_2Cl_2 (20 mL), and the water was extracted with CH_2Cl_2 (3 × 10 mL). The organic solvents were combined and removed under reduced pressure to yield a yellow solid. Chromatographic separation (petroleum ether−ethyl acetate, 5:1) gave the title compounds.

*(E)-N-(2-Methoxy-5-(3-(5-methoxy-2,2-dimethyl-2H-chromen-8-yl)-3-oxoprop-1-en-1-yl)phenyl)acetamide (**9h**).* **9h** was obtained from **8** and acetic acid as described for method B: 387 mg, 95% yield as a yellow solid; mp 169−171 °C. ^{1}H NMR (400 MHz, $CDCl_3$) δ: 8.76 (s, 1H), 7.76 (s, 1H), 7.70 (d, J = 8.8 Hz, 1H), 7.66 (s, 2H), 7.25 (d, J = 8.4 Hz, 1H), 6.87 (d, J = 8.4 Hz, 1H), 6.68 (d, J = 10.0 Hz, 1H), 6.50 (d, J = 8.8 Hz, 1H), 5.63 (d, J = 10.0 Hz, 1H), 3.91 (s, 3H), 3.87 (s, 3H), 2.21 (s, 3H), 1.55 (s, 6H). ^{13}C NMR (100 MHz, DMSO-d_6) δ: 188.28, 168.67, 157.90, 152.74, 151.14, 141.43, 131.19, 129.50, 128.11, 127.07, 126.09, 124.65, 121.01, 119.46, 115.95, 111.30, 109.86, 104.23, 76.92, 55.95, 55.90, 27.36, 23.93. MS (ESI, m/z): 430.20 $[M + Na]^+$.

*(E)-N-(2-Methoxy-5-(3-(5-methoxy-2,2-dimethyl-2H-chromen-8-yl)-3-oxoprop-1-en-1-yl)phenyl)propionamide (**9i**).* **9i** was obtained from **8** and propionic acid as described for method B: 366 mg, 87% yield as a yellow solid; mp 138−140 °C. ^{1}H NMR (400 MHz, $CDCl_3$) δ: 8.80 (s, 1H), 7.75 (s, 1H), 7.69 (d, J = 8.8 Hz, 1H), 7.65 (s, 2H), 7.25 (d, J = 8.4 Hz, 1H), 6.88 (d, J = 8.4 Hz, 1H), 6.68 (d, J = 10.0 Hz, 1H), 6.50 (d, J = 8.8 Hz, 1H), 5.63 (d, J = 10.0 Hz, 1H), 3.92 (s, 3H), 3.88 (s, 3H), 2.43 (q, J = 7.5 Hz, 2H), 1.54 (s, 6H), 1.25 (t, J = 7.4 Hz, 3H). ^{13}C NMR (100 MHz, DMSO-d_6) δ: 188.20, 172.34, 157.90, 152.77, 151.26, 141.41, 131.22, 129.51, 128.03, 127.05, 126.04, 124.65, 120.97, 119.71, 115.95, 111.29, 109.85, 104.22, 76.94, 55.94, 55.90, 29.25, 27.33, 9.73. MS (ESI, m/z): 444.22 $[M + Na]^+$.

*(E)-N-(2-Methoxy-5-(3-(5-methoxy-2,2-dimethyl-2H-chromen-8-yl)-3-oxoprop-1-en-1-yl)phenyl)acrylamide (**9j**).* **9j** was obtained from **8** and acrylic acid as described for method B: 373 mg, 89% yield as a yellow solid; mp 123−125 °C. ^{1}H NMR (400 MHz, $CDCl_3$) δ: 8.89 (s, 1H), 7.86 (s, 1H), 7.70 (d, J = 8.8 Hz, 1H), 7.66 (s, 2H), 7.29 (d, J = 8.8 Hz, 1H), 6.90 (d, J = 8.5 Hz, 1H), 6.68 (d, J = 10.0 Hz, 1H), 6.51 (d, J = 8.8 Hz, 1H), 6.42 (d, J = 16.8 Hz, 1H), 6.29 (dd, J = 16.8, 10.1 Hz, 1H), 5.77 (d, J = 10.1 Hz, 1H), 5.63 (d, J = 10.0 Hz, 1H), 3.94 (s, 3H), 3.88 (s, 3H), 1.55 (s, 6H). ^{13}C NMR (100 MHz, DMSO-d_6) δ: 188.28, 163.45, 157.90, 152.76, 151.45, 141.33, 131.88, 131.20, 129.53, 127.71, 127.10, 126.85, 126.37, 124.79, 120.98, 120.11, 115.94, 111.44, 109.85, 104.23, 76.94, 55.99, 55.95, 27.33. MS (ESI, m/z): 420.23 $[M + H]^+$.

*(E)-N-(2-Methoxy-5-(3-(5-methoxy-2,2-dimethyl-2H-chromen-8-yl)-3-oxoprop-1-en-1-yl)phenyl)pentanamide (**9k**).* **9k** was obtained from **8** and pentanoic acid as described for method B: 373 mg, 83% yield

as a yellow solid; mp 97−99 °C. ^{1}H NMR (400 MHz, $CDCl_3$) δ: 8.80 (s, 1H), 7.73 (s, 1H), 7.70 (d, J = 8.8 Hz, 1H), 7.65 (s, 2H), 7.24 (s, 1H), 6.88 (d, J = 8.4 Hz, 1H), 6.68 (d, J = 10.0 Hz, 1H), 6.50 (d, J = 8.8 Hz, 1H), 5.63 (d, J = 10.0 Hz, 1H), 3.92 (s, 3H), 3.88 (s, 4H), 2.40 (t, J = 7.5 Hz, 2H), 1.77−1.67 (m, 2H), 1.54 (s, 6H), 1.42 (dd, J = 15.3, 7.7 Hz, 2H), 0.95 (t, J = 7.3 Hz, 3H). ^{13}C NMR (100 MHz, DMSO-d_6) δ: 188.13, 171.63, 157.92, 152.78, 151.32, 141.37, 131.25, 129.47, 128.03, 127.05, 126.23, 124.61, 120.96, 119.64, 115.96, 111.27, 109.85, 104.22, 76.93, 55.93, 55.89, 35.74, 27.38, 27.32, 21.73, 13.75. MS (ESI, m/z): 472.25 $[M + Na]^+$.

*(E)-N-(2-Methoxy-5-(3-(5-methoxy-2,2-dimethyl-2H-chromen-8-yl)-3-oxoprop-1-en-1-yl)phenyl)isobutyramide (**9l**).* **9l** was obtained from **8** and isobutyric acid as described for method B: 361 mg, 83% yield as a yellow solid; mp 113−115 °C. ^{1}H NMR ($CDCl_3$, 400 MHz) δ: 1.32 (s, 3H), 1.34 (s, 3H), 1.49 (s, 6H), 2.85 (qui, 1H, J = 7.6 Hz), 3.86 (s, 3H), 3.88(s, 3H), 5.62 (d, 1H, J = 10.0 Hz), 6.50 (d, 1H, J = 8.8 Hz), 6.68 (d, 1H, J = 10.0 Hz), 6.96 (d, 1H, J = 8.4 Hz), 7.27−7.29 (m, 1H), 7.41(d, 1H, J = 8.80 Hz), 7.59−7.61 (m, 2H), 7.70 (d, 1H, J = 8.8 Hz). MS (ESI, m/z): 436.25 $[M + H]^+$.

*(E)-1-(2-Methoxy-5-(3-(5-methoxy-2,2-dimethyl-2H-chromen-8-yl)-3-oxoprop-1-en-1-yl)phenyl)urea (**9m**). General Procedures of Method C.* To **8** (197 mg, 0.54 mmol) in AcOH (6.8 mL) was added KOCN (131 mg, 1.62 mmol) and water (0.54 mL) and stirred at room temperature overnight. When the reaction was finished, the solvent was removed under vocum and the residue was purified by flash chromatograph using petroleum ether/ethyl acetate (3:1) as eluent to give the title compound **9m** (163 mg, 74% yield as a yellow solid); mp 227−229 °C. ^{1}H NMR (400 MHz, $CDCl_3$) δ: 8.40 (s, 1H), 7.70 (d, J = 8.8 Hz, 1H), 7.65 (s, 2H), 7.23 (d, J = 8.6 Hz, 1H), 6.98 (s, 1H), 6.87 (d, J = 8.4 Hz, 1H), 6.68 (d, J = 10.0 Hz, 1H), 6.51 (d, J = 8.8 Hz, 1H), 5.63 (d, J = 10.0 Hz, 1H), 3.89 (s, 3H), 3.88 (s, 3H), 1.54 (s, 6H). ^{13}C NMR (100 MHz, DMSO-d_6) δ: 188.28, 157.88, 155.90, 152.72, 149.37, 142.07, 131.22, 130.15, 129.53, 127.24, 124.22, 123.82, 121.06, 115.96, 115.27, 110.60, 109.85, 104.21, 76.92, 55.92, 55.91, 27.35.MS (ESI, m/z): 431.21 $[M + Na]^+$.

*(E)-N-(2-Methoxy-5-(3-(5-methoxy-2,2-dimethyl-2H-chromen-8-yl)-3-oxoprop-1-en-1-yl)phenyl)-2-(3-(trifluoromethyl)phenyl)-acetamide (**9n**).* **9n** was obtained from **8** and 2-(3-(trifluoromethyl)-phenyl)acetic acid as described for method B: 430 mg, 78% yield as a yellow solid; mp 70−72 °C. ^{1}H NMR (400 MHz, $CDCl_3$) δ: 8.75 (s, 1H), 7.65 (s, 1H), 7.70 (d, J = 8.8 Hz, 1H), 7.65−7.48 (m, 6H), 7.23 (d, J = 8.4 Hz, 1H), 6.83 (d, J = 8.8 Hz, 1H), 6.68 (d, J = 10.0 Hz, 1H), 6.50 (d, J = 8.8 Hz, 1H), 5.63 (d, J = 10.0 Hz, 1H), 3.87 (s, 3H), 3.82 (s, 2H), 3.81 (s, 3H), 1.53 (s, 6H). ^{13}C NMR (100 MHz, DMSO-d_6) δ: 188.05, 168.89, 157.95, 152.78, 151.43, 141.17, 137.46, 133.36, 131.27, 129.33, 129.20, 127.71, 127.13, 126.64, 125.78, 125.75, 124.72, 123.26, 123.22, 120.92, 119.63, 116.00, 111.39, 109.84, 104.22, 76.85, 55.96, 55.91, 42.23, 27.18. MS (ESI, m/z): 574.26 $[M + Na]^+$.

General Procedures of Method D for the Synthesis of 9o−9r. To **8** (365 mg, 1 mmol) in CH_2Cl_2 (5 mL) was added RSO_2Cl (2 equiv) and Et_3N (2 equiv) and stirred at room temperature for 6 h. When completed, the solvent was removed under vacuum and the residue was purified by flash chromatograph using petroleum ether/ethyl acetate (5:1) as eluent to give the title compounds.

*(E)-N-(2-Methoxy-5-(3-(5-methoxy-2,2-dimethyl-2H-chromen-8-yl)-3-oxoprop-1-en-1-yl)phenyl)methanesulfonamide (**9o**).* **9o** was obtained from **8** and methanesulfonyl chloride as described for method D: 341 mg, 77% yield as a yellow solid; mp 125−127 °C. ^{1}H NMR (400 MHz, $CDCl_3$) δ 7.88 (s, 1H), 7.72 (d, J = 9.0 Hz, 1H), 7.69 (d, J = 16 Hz, 1H), 7.64 (d, J = 16 Hz, 1H), 7.33 (d, J = 8.3 Hz, 1H), 6.93 (d, J = 8.4 Hz, 1H), 6.88 (s, 1H), 6.68 (d, J = 10.0 Hz, 1H), 6.52 (d, J = 8.9 Hz, 1H), 5.64 (d, J = 10.0 Hz, 1H), 3.93 (s, 3H), 3.88 (s, 3H), 2.98 (s, 3H), 1.54 (s, 6H). ^{13}C NMR (100 MHz, DMSO-d_6) δ: 188.28, 157.93, 153.91, 152.74, 140.77, 131.22, 129.43, 127.84, 127.50, 126.61, 125.01, 123.32, 120.97, 115.95, 112.22, 109.82, 104.23, 76.90, 56.03, 55.95, 27.42. MS (ESI, m/z): 466.15 $[M + Na]^+$.

*(E)-N-(2-Methoxy-5-(3-(5-methoxy-2,2-dimethyl-2H-chromen-8-yl)-3-oxoprop-1-en-1-yl)phenyl)cyclopropanesulfonamide (**9p**).* **9p** was obtained from **8** and cyclopropanesulfonyl chloride as described for method D: 352 mg, 75% yield as a yellow solid; mp 123−125 °C. ^{1}H NMR (400 MHz, $CDCl_3$) δ: 7.92 (s, 1H), 7.72 (d, J = 8.9 Hz, 1H), 7.69 (d, J = 16 Hz, 1H), 7.64 (d, J = 16 Hz, 1H), 7.32 (d, J = 8.2 Hz, 1H), 6.92 (d, J = 8.4 Hz, 1H), 6.84 (s, 1H), 6.68 (d, J = 10.0 Hz, 1H), 6.52 (d, J = 8.9 Hz, 1H), 5.64 (d, J = 10.0 Hz, 1H), 3.93 (s, 3H), 3.88 (s, 3H), 2.51−2.43 (m, 1H), 1.54 (s, 6H), 0.96−0.82 (m, 4H). ^{13}C NMR (100 MHz, DMSO-d_6) δ: 188.30, 157.92, 154.24, 152.73, 140.82, 131.21, 129.43, 127.86, 127.37, 126.75, 124.95, 123.47, 120.99, 115.95, 112.07, 109.82, 104.23, 76.89, 56.04, 55.95, 30.11, 27.40, 4.88. MS (ESI, m/z): 470.18 $[M + H]^+$.

*(E)-N-(2-Methoxy-5-(3-(5-methoxy-2,2-dimethyl-2H-chromen-8-yl)-3-oxoprop-1-en-1-yl)phenyl)-4-methylbenzenesulfonamide (**9q**).* **9q** was obtained from **8** and TsCl as described for method D: 446 mg, 86% yield as a yellow solid; mp 155−157 °C. ^{1}H NMR (400 MHz, $CDCl_3$) δ: 7.88 (s, 1H), 7.72 (d, J = 8.8 Hz, 1H), 7.67 (d, J = 16 Hz, 1H), 7.64 (d, J = 7.6 Hz, 2H), 7.60 (d, J = 16 Hz, 1H), 7.24 (d, J = 8.4 Hz, 1H), 7.18 (d, J = 8 Hz, 2H), 7.05 (s, 1H), 6.74 (d, J = 8.4 Hz, 1H), 6.69 (d, J = 10 Hz, 1H), 6.52 (d, J = 8.8 Hz, 1H), 5.65 (d, J = 10 Hz, 1H), 3.88 (s, 3H), 3.69 (s, 3H), 2.34 (s, 3H), 1.56 (s, 6H). ^{13}C NMR (100 MHz, DMSO-d_6) δ: 188.30, 157.94, 153.85, 152.73, 142.93, 140.70, 137.38, 131.21, 129.44, 129.23, 128.06, 127.29, 126.61, 126.13, 124.97, 123.19, 120.98, 115.97, 112.10, 109.83, 104.23, 76.88, 55.95, 55.70, 27.41, 20.88. MS (ESI, m/z): 542.20 $[M + Na]^+$.

*(E)-N-(2-Methoxy-5-(3-(5-methoxy-2,2-dimethyl-2H-chromen-8-yl)-3-oxoprop-1-en-1-yl)phenyl)-1-phenylmethanesulfonamide (**9r**).* **9r** was obtained from **8** and phenylmethanesulfonyl chloride as described for method D: 431 mg, 83% yield as a yellow solid; mp 137−139 °C. ^{1}H NMR (400 MHz, $CDCl_3$) δ: 7.90 (s, 1H), 7.74 (d, J = 8.8 Hz, 1H), 7.67 (d, J = 16.2 Hz, 1H), 7.63 (d, J = 16.2 Hz, 1H), 7.33−7.28 (m, 4H), 7.18 (d, J = 6.9 Hz, 2H), 6.89 (d, J = 8.4 Hz, 1H), 6.76 (s, 1H), 6.70 (d, J = 10.0 Hz, 1H), 6.53 (d, J = 8.8 Hz, 1H), 5.65 (d, J = 10.0 Hz, 1H), 4.33 (s, 2H), 3.90 (s, 3H), 3.81 (s, 3H), 1.56 (s, 6H). ^{13}C NMR (100 MHz, DMSO-d_6) δ: 188.48, 157.88, 153.36, 152.69, 140.91, 131.14, 130.96, 129.57, 129.48, 128.19, 128.10, 127.40, 127.29, 126.76, 125.00, 122.61, 121.06, 115.95, 112.06, 109.83, 104.21, 76.87, 58.13, 55.95, 27.43. MS (ESI, m/z): 542.27 $[M + Na]^+$.

General Procedures of Method D for the Synthesis of 9s and 9t. First, the compound **8** was act with the Boc-amino acid as the method B, then the result compound was dissolved in CH_2Cl_2/CF_3COOH (1:1, 3 mL), stirred at room temperature, as the reaction was completed, the solvent was removed under vacuum, and the residue was purified by flash chromatograph using petroleum ether/ethyl acetate (5:1) as eluent to give the title compounds.

*(E)-2-Amino-N-(2-methoxy-5-(3-(5-methoxy-2,2-dimethyl-2H-chromen-8-yl)-3-oxoprop-1-en-1-yl)phenyl)acetamide (**9s**).* **9s** was obtained from **8** and Boc-Gly as described for method E: 329 mg, 78% yield as a yellow solid; mp 120−122 °C. ^{1}H NMR (400 MHz, DMSO-d_6) δ: 8.81 (d, J = 1.8 Hz, 1H), 7.59 (d, J = 15.6 Hz, 1H), 7.58 (d, J = 8.8 Hz, 1H), 7.54 (d, J = 15.6 Hz, 1H), 7.37 (dd, J = 8.5, 2.0 Hz, 1H), 7.15 (d, J = 8.5 Hz, 1H), 6.72 (d, J = 8.9 Hz, 1H), 6.62 (d, J = 10.0 Hz, 1H), 5.79 (d, J = 10.0, 1H), 3.93 (s, 3H), 3.87 (s, 3H), 3.29 (s, 2H), 1.51 (s, 6H). ^{13}C NMR (100 MHz, DMSO-d_6) δ: 196.79, 171.24, 166.53, 157.94, 152.79, 141.45, 132.07, 131.24, 129.51, 128.76, 127.89, 120.98, 118.38, 115.95, 109.87, 104.22, 76.96, 65.80, 56.12, 55.9, 44.87, 27.36, 27.33. MS (ESI, m/z): 423.31 $[M + H]^+$.

*(R,E)-2-Amino-N-(2-methoxy-5-(3-(5-methoxy-2,2-dimethyl-2H-chromen-8-yl)-3-oxoprop-1-en-1-yl)phenyl)propanamide (**9t**).* **9t** was obtained from **8** and D-Boc-Ala as described for method E: 340 mg, 78% yield as a yellow solid; mp 133−135 °C. ^{1}H NMR (400 MHz, $CDCl_3$) δ 9.79 (s, 1H), 8.82 (d, J = 1.9 Hz, 1H), 7.69 (d, J = 8.8 Hz, 1H), 7.65 (s, 2H), 7.28 (d, J = 2.1 Hz, 1H), 6.88 (d, J = 8.5 Hz, 1H), 6.68 (d, J = 10.0 Hz, 1H), 6.50 (d, J = 8.9 Hz, 1H), 5.62 (d, J = 10.0 Hz, 1H), 3.93 (s, 3H), 3.88 (s, 3H), 3.70 (q, J = 7.5 Hz, 1H), 1.54 (s, 6H), 1.45 (d, J = 7.0 Hz, 3H). ^{13}C NMR (100 MHz, DMSO-d_6) δ: 188.18, 174.24, 157.93, 152.80, 150.14, 141.42, 131.23, 129.53, 127.95, 127.33, 125.79, 124.73, 120.95, 116.26, 115.93, 111.08, 109.87, 104.23, 76.96, 56.13, 55.94, 50.83, 27.34, 20.91. MS (ESI, m/z): 437.33 $[M + H]^+$.

Biological Assay Methods. *Antiproliferative Assays.* Human leukemia cells (K562), rat colon carcinoma (C26), and human colon carcinoma (HCT116, DLD-1, HCT15, HCT-8 and HCT-8/T) cells were grown in RPMI-1640 medium, (Gibco, Milano, Italy). Human

dx.doi.org/10.1021/jm500849z | J. Med. Chem. 2014, 57, 7977−7989

hepatocellular carcinoma (HepG2), human melanoma (A375), human lung carcinoma (NCI-H358), human breast carcinoma (MCF-7 and MCF-7/ADR), human ovarian carcinoma (ES-2, A2780S, A2780/T and A2780/CP), human stomach carcinoma (AGS), and human glioma carcinoma (U251) cells were incubated in DMEM (Gibco, Milano, Italy). Both media contained 10% fetal bovine serum (FBS) (Invitrogen, Milano, Italy), 100 units/mL penicillin (Gibco, Milano, Italy), and 100 μg/mL streptomycin (Gibco, Milano, Italy). Cells were incubated at 37 °C in a humidified atmosphere of 5% CO_2. These cells (1000 cells/well) were seeded on 96-well plates and incubated overnight. Selected compounds were added at various doses and incubated for 48 h. MTT was then added for 4 h incubation. The MTT formazan precipitate was then dissolved in 150 mL of DMSO, and the absorbance was measured at a wavelength of 590 nm.

Flow Cytometry. HepG2 cells were treated with various concentrations of selected compound or DMSO vehicle for 24 or 48 h at 37 °C. Then cells were stained with 5 mg/mL PI containing 10 mg/mL of DNase-free RNase to analyze cell cycle, or stained with Annexin V-FITC/PI to measure cell apoptosis. After treatment, the cells were analyzed by flow cytometer (TASC240, USA).

Immunofluorescence Assay. HepG2 cells (1×10^4) were seeded in 96-well culture plate and incubated overnight. Cells were treatment with DMSO or **8** for 24 h. Then cells were fixed with methanol and blocked for 45 min in 5% BSA/PBS. The cells were incubated overnight with primary antibody (α-tubulin) at 4 °C. After washing three times with PBS, cells were incubated with corresponding fluorescence-conjugated secondary antibody for 1 h. The nuclei of cells were labeled with DAPI. Cells were visualized using a fluorescence microscopy.

In Vitro Tubulin Polymerization Assay. Two mg/mL tubulin (Cytoskeleton) was resuspended in PEM buffer [80 mM PIPES, (pH 6.9), 0.5 mM EGTA, 2 mM $MgCl_2$, and 15% glycerol] and then was preincubated with compounds or vehicle DMSO on ice. PEG containing GTP was added to the final concentration of 1 mM before detecting the tubulin polymerization reaction. The reaction was monitored by a spectrophotometer in absorbance at 340 nm at 37 °C every 30 s. The final concentrations of the compound were list as follow: **8** (0.5, 2, 5 μM), colchicine (2 μM).

Molecular Docking. Tubulin was chosen as the target receptor. The 3D structure of the receptor was gained from Protein Data Bank (PDBs 3E22 and 3HKD). Molecule **8** was built with ChemBio3D and optimized at molecular mechanical and semiempirical level by using Hyperchem[2] software. The structure of colchicine and TN-16 were directly extracted from the crystal structure of complex 1 composed of tubulin and colchicines. Conformers of colchicine/TN-16 and the compound **8** were created by the aid of Omega, and the up limit of conformer number was set to 2000. Then these molecules were docked to the binding site of tubulin by employing a protein−ligand docking program FRED. Scoring function chemgauss3 was used for exhaustive searching, solid body optimizing, and interaction scoring.

Determination of Maximum Tolerated Dose (MTD). Animals: BALB/c mice (SPF), 18−22 g, 6−8 weeks years old, female and male were half and half. Acute toxicity information was obtained from short-duration dose-ranging studies that define as MTD. It was used to determine the largest dose possible before one death occurred in the test animals. Different doses of the substance were administered to the animals intravenously ($n = 4$). Survival and adverse effects of each animal were recorded every other day after administration.

Wound Healing Assay. Human umbilical vascular endothelial cells (HUVEC) were incubated in DMEM medium. Cells were allowed to grow into full confluence in 6-well plates and then incubated without FBS for 16 h to inactivate cells. Monolayer cells were wounded by scratching with a pipet tips and washed with PBS. Fresh DMEM containing vehicle or different concentrations of compound **8** was added to the scratched monolayers. After treating for 24 h, the images were taken by fluorescence microscope (Carl Zeiss Microimaging Inc.). The cells were quantified by manual counting, and the percentage of migrated cells inhibited by compound **8** was expressed on the basis of vehicle wells.

Tube Formation Assay. The tube formation assay was conducted as described previously (Liang Ma et al. 2011). BD Matrigel matrix (BD Biosciences) were thawed at 4 °C for overnight, and HUVECs ($2-4 \times 10^4$) suspended in DMEM were seeded in 96-well culture plates after polymerization of the Matrigel at 37 °C for 30 min. They were then treated with different concentrations of compound **8** or vehicle. After 6−8 h, cells were photographed with a digital camera attached to an inverted microscope (Carl Zeiss Microimaging Inc.).

In Vivo Tumor Models. For every tumor xenograft model, the mice were randomly assigned to groups. We used 5−6-week-old female Balb/C and athymic nude mice, respectively, implanted the indicated number of cells suspended in 100 CE HBSS in the right flank of mice. When tumor volumes reached 100 mm^3, the animals were treated with vehicle (2.5% Tween-80 and 2.5% ethanol) and **8·HCl** (10 mg/kg) every 2 days. Signs of toxicity and mortality were observed daily. Tumor volumes and body weights were measured every 2 days when administrated with a caliper (calculated volume (mm^3) = $\pi/6 \times$ length $\times$ width $\times$ width). The antitumor activity of compound was evaluated by tumor inhibitor = (1 − tumor weight of treated-group/tumor weight of control group) × 100%.

Ethics statement: Animal studies were conducted in conformity with the Institutional Guide for the Care and Use of Laboratory Animals. All mouse protocols were approved by the Animal Care and Use Committee of Sichuan University (Chengdu, Sichuan, China).

AUTHOR INFORMATION

Corresponding Author

*Phone: +86-28-85164063. Fax: +86-28-85164060. E-mail: chenlijuan125@163.com.

Author Contributions

‖These authors contributed equally and should be considered as co-first authors

Notes

The authors declare no competing financial interest.

ACKNOWLEDGMENTS

The authors greatly appreciate the financial support from National Key Programs of China during the 12th Five-Year Plan Period (2012ZX09103101-009) and National Natural Science Foundation of China (81373283).

ABBREVIATIONS USED

DBU, 1,8-diazabicyclo[5,4,0]-undec-7-ene; TLC, thin layer chromatography; MTT, 3-(4,5-dimethylthiazol-2-yl)-2,5-diphenyltetrazolium bromide; DHP, 3,4-dihydro-2*H*-pyran; GTP, guanosine triphosphate; DMSO, dimethyl sulfoxide; Gly, glycine; Ala, alanine

REFERENCES

(1) Amos, L. A. Microtubule structure and its stabilisation. *Org. Biomol. Chem.* **2004**, *2*, 2153−2160.

(2) Walczak, C. E. Microtubule dynamics and tubulin interacting proteins. *Curr. Opin. Cell Biol.* **2000**, *12*, 52−56.

(3) Downing, K. H.; Nogales, E. Tubulin structure: insights into microtubule properties and functions. *Curr. Opin. Struct. Biol.* **1998**, *8*, 785−791.

(4) Dumontet, C.; Jordan, M. A. Microtubule-binding agents: a dynamic field of cancer therapeutics. *Nature Rev. Drug Discovery* **2010**, *9*, 790−803.

(5) Perez, E. A. Microtubule inhibitors: differentiating tubulin-inhibiting agents based on mechanisms of action, clinical activity, and resistance. *Mol. Cancer Ther.* **2009**, *8*, 2086−2095.

(6) Yue, Q. X.; Liu, X.; Guo, D. A. Microtubule-binding natural products for cancer therapy. *Planta Med.* **2010**, *76*, 1037−1043.

(7) Jordan, M. A.; Wilson, L. Microtubules as a target for anticancer drugs. *Nature Rev. Cancer* **2004**, *4*, 253−265.

(8) Löwe, J.; Li, H.; Downing, K. H.; Nogales, E. Refined structure of αβ-tubulin at 3.5 Å resolution. *J. Mol. Biol.* **2001**, *313*, 1045−1057.

(9) Gigant, B.; Wang, C.; Ravelli, R. B.; Roussi, F.; Steinmetz, M. O.; Curmi, P. A.; Sobel, A.; Knossow, M. Structural basis for the regulation of tubulin by vinblastine. *Nature* **2005**, *435*, 519−522.
(10) Kavallaris, M.; Verrills, N. M.; Hill, B. T. Anticancer therapy with novel tubulin-interacting drugs. *Drug Resist. Updates* **2001**, *4*, 392−401.
(11) Wu, W.; Ye, H.; Wan, L.; Han, X.; Wang, G.; Hu, J.; Tang, M.; Duan, X.; Fan, Y.; He, S.; Huang, L.; Pei, H.; Wang, X.; Li, X.; Xie, C.; Zhang, R.; Yuan, Z.; Mao, Y.; Wei, Y.; Chen, L. Millepachine, a novel chalcone, induces G2/M arrest by inhibiting CDK1 activity and causing apoptosis via ROS-mitochondrial apoptotic pathway in human hepatocarcinoma cells in vitro and in vivo. *Carcinogenesis* **2013**, *34*, 1636−1643.
(12) Cao, D.; Han, X.; Wang, G.; Yang, Z.; Peng, F.; Ma, L.; Zhang, R.; Ye, H.; Tang, M.; Wu, W.; Lei, K.; Wen, J.; Chen, J.; Qiu, J.; Liang, X.; Ran, Y.; Sang, Y.; Xiang, M.; Peng, A.; Chen, L. Synthesis and biological evaluation of novel pyranochalcone derivatives as a new class of microtubule stabilizing agents. *Eur. J. Med. Chem.* **2013**, *62*, 579−589.
(13) Wang, G.; Li, C.; He, L.; Lei, K.; Wang, F.; Pu, Y.; Yang, Z.; Cao, D.; Ma, L.; Chen, J.; Sang, Y.; Liang, X.; Xiang, M.; Peng, A.; Wei, Y.; Chen, L. Design, synthesis and biological evaluation of a series of pyrano chalcone derivatives containing indole moiety as novel anti-tubulin agents. *Bioorg. Med. Chem.* **2014**, *22*, 2060−2079.
(14) Wang, G.; Peng, F.; Cao, D.; Yang, Z.; Han, X.; Liu, J.; Wu, W.; He, L.; Ma, L.; Chen, J.; Sang, Y.; Xiang, M.; Peng, A.; Wei, Y.; Chen, L. Design, synthesis and biological evaluation of millepachine derivatives as a new class of tubulin polymerization inhibitors. *Bioorg. Med. Chem.* **2013**, *21*, 6844−6854.
(15) Wang, G.; Wu, W.; Peng, F.; Cao, D.; Yang, Z.; Ma, L.; Qiu, N.; Ye, H.; Han, X.; Chen, J.; Qiu, J.; Sang, Y.; Liang, X.; Ran, Y.; Peng, A.; Wei, Y.; Chen, L. Design, synthesis, and structure−activity relationship studies of novel millepachine derivatives as potent anti-proliferative agents. *Eur. J. Med. Chem.* **2012**, *54*, 793−803.
(16) Szakacs, G.; Paterson, J. K.; Ludwig, J. A.; Booth-Genthe, C.; Gottesman, M. M. Targeting multidrug resistance in cancer. *Nature Rev. Drug Discovery* **2006**, *5*, 219−234.
(17) Baguley, B. C. Multiple drug resistance mechanisms in cancer. *Mol. Biotechnol.* **2010**, *46*, 308−316.
(18) Kavallaris, M. Microtubules and resistance to tubulin-binding agents. *Nature Rev. Cancer* **2010**, *10*, 194−204.
(19) Ganguly, A.; Cabral, F. New insights into mechanisms of resistance to microtubule inhibitors. *Biochim. Biophys. Acta* **2011**, *1816*, 164−171.
(20) Xiao, M.; Ahn, S.; Wang, J.; Chen, J. J.; Miller, D. D.; Dalton, J. T.; Li, W. Discovery of 4-aryl-2-benzoyl-imidazoles as tubulin polymerization inhibitor with potent antiproliferative properties. *J. Med. Chem.* **2013**, *56*, 3318−3329.
(21) Canela, M.; Pérez-Pérez, M.; Sáez-Calvo, G.; Díaz, F.; Camarasa, M.; Liekens, S.; Priego, E. Novel colchicine-site binders with a cyclohexanedione scaffold identified through a ligand-based virtual screening approach. *J. Med. Chem.* **2014**, *57*, 3924−3938.
(22) Kim, D. Y.; Kim, K.-H.; Kim, N. D.; Lee, K. Y.; Han, C. K.; Yoon, J. H.; Moon, S. K.; Lee, S. S.; Seong, B. L. Design and biological evaluation of novel tubulin inhibitors as antimitotic agents using a pharmacophore binding model with tubulin. *J. Med. Chem.* **2006**, *49*, 5664−5670.
(23) Ducki, S.; Rennison, D.; Woo, M.; Kendall, A.; Chabert, J. F.; McGown, A. T.; Lawrence, N. J. Combretastatin-like chalcones as inhibitors of microtubule polymerization. Part 1: synthesis and biological evaluation of antivascular activity. *Bioorg. Med. Chem.* **2009**, *17*, 7698−7710.
(24) Paulekuhn, G. S.; Dressman, J. B.; Saal, C. Trends in active pharmaceutical ingredient salt selection based on analysis of the orange book database. *J. Med. Chem.* **2007**, *50*, 6665−6672.
(25) Skwarczynski, M.; Hayashi, Y.; Kiso, Y. Paclitaxel prodrugs: toward smarter delivery of anticancer agents. *J. Med. Chem.* **2006**, *49*, 7253−7269.